

# **Modulation of the cellular organelle specificity in Re(I) tetrazolato complexes leads to unprecedented phosphorescent labeling of lipid droplets\*\***

Christie A. Bader,<sup>a</sup> Robert D. Brooks,<sup>a</sup> Yeap S. Ng,<sup>a</sup> Alexandra Sorvina,<sup>a</sup> Melissa V. Werrett,<sup>b</sup> Phillip J. Wright,<sup>b</sup> Ayad G. Anwer,<sup>c</sup> Douglas A. Brooks,<sup>a</sup> Stefano Stagni,<sup>d</sup> Sara Muzzioli,<sup>d</sup> Morry Silberstein,<sup>b</sup> Brian W. Skelton,<sup>e</sup> Ewa M. Goldys,<sup>c</sup> Sally E. Plush,<sup>a</sup> Tetyana Shandala,<sup>\*,a</sup> Massimiliano Massi<sup>\*,b</sup>

<sup>a</sup> *School of Pharmacy and Medical Science, University of South Australia, Adelaide 5001 SA, Australia*

<sup>b</sup> *Department of Chemistry, Curtin University, Bentley 6102 WA, Australia*

<sup>c</sup> *Department of Physics and Astronomy, Macquarie University, North Ryde 2109 NSW, Australia*

<sup>d</sup> *Department of Industrial Chemistry, University of Bologna, Bologna 40126, Italy*

<sup>e</sup> *Centre for Microscopy, Characterisation and Analysis, University of Western Australia, Crawley 6009 WA, Australia*

Corresponding author Email: Tetyana.Shandala@unisa.edu.au; M.Massi@curtin.edu.au.

The development of organelle-specific dyes for biomedical research has become an area of increasing interest. Metal complexes emitting from triplet metal-to-ligand charge transfer states (<sup>3</sup>MLCT) have recently emerged as a promising alternative to conventional fluorescent probes.<sup>[1-4]</sup> The goal is to overcome the apparent shortcomings of organic-based fluorescent probes such as self-quenching, photo-bleaching and signal discrimination versus endogenous autofluorescence (e.g. emission from species such as flavins). Families of luminescent Re(I),<sup>[5-7]</sup> Ru(II),<sup>[8,9]</sup> Ir(III),<sup>[10-12]</sup> Pt(II),<sup>[13]</sup> Au(I)<sup>[14]</sup>, Au(III)<sup>[15]</sup> and trivalent lanthanoid<sup>[16-18]</sup> complexes have potentially shown significant advantages as cellular labels. A challenge in the field, however, is to define a structure-activity relationship that will allow a direct link between the chemical nature of a complex and its biological activity in terms of cellular permeability and organelle targeting.<sup>[19,20]</sup> An understanding of this relationship is of critical importance for the rational design of a chemical structure that encompasses and optimizes chemical properties (e.g. solubility and lipophilicity), photophysical characteristics (absorption/emission energy and photoluminescent quantum yield) and biological

behavior (targeting to specific cellular compartments, cell types or discrimination between healthy and diseased cells). While some aspects of this rationalization have been pursued by covalently linking non-specific phosphorescent metal complexes to biological vectors such as sugars or oligopeptides,<sup>[7,9,21-25]</sup> comparably less information is available for non-bioconjugated metal complexes.<sup>[26]</sup>

Preliminary guidelines to govern the cellular uptake and specificity of tricarbonyl diimine Re(I) complexes through modification of their chemical nature have started to emerge.<sup>[19]</sup> The majority of the studies, however, have been carried out on cationic complexes. Meanwhile, the behavior of analogous neutral non-bioconjugated complexes has received scarce attention. Hence, the structure-activity relationship for neutral complexes of the type *fac*-[Re(CO)<sub>3</sub>(diim)**L**], where diim is a bidentate ligand and **L** represents an anionic donor species, requires further investigation. Aiming to extend the structure-activity studies to neutral Re(I) complexes, we have recently investigated cellular uptake and organelle targeting of neutral Re(I) tetrazolato complexes, the structures of which are shown in Figure 1.

The complexes **1** and **2** are reported, with the difference being that in complex **2** the pyridine ring is capable of undergoing protonation equilibrium at physiological pH. Our results indeed show that the two complexes have well differentiated organelle targeting. Remarkably, complex **1** was found to exhibit high specificity for the lipid droplets of live human and *Drosophila* adipose cells. These spherical organelles store neutral triglycerides and while in the past they were simplistically considered to function as lipid storage, it is now established that they have fundamental roles in the regulation of cellular metabolism<sup>[27,28]</sup> and in the development of a number of key human diseases, including diabetes, neutral lipid storage disease (NLSD) as well as associated cardiomyopathies.<sup>[29,30]</sup> However, a comprehensive understanding of the cellular function of the lipid droplets is yet to be uncovered.<sup>[31-34]</sup> The need to improve our understanding of these organelles makes efficient stains for lipid droplets a highly desirable tool. In this respect and to the best of our knowledge, our result represents the first example of a metal-based phosphorescent probe specifically recognizing this vital organelle in live mammalian and insect cells. This is significant because staining of adipose cells is currently achieved with the exclusive use of fluorescent labels, consequently suffering from the previously listed drawbacks.<sup>[35]</sup>

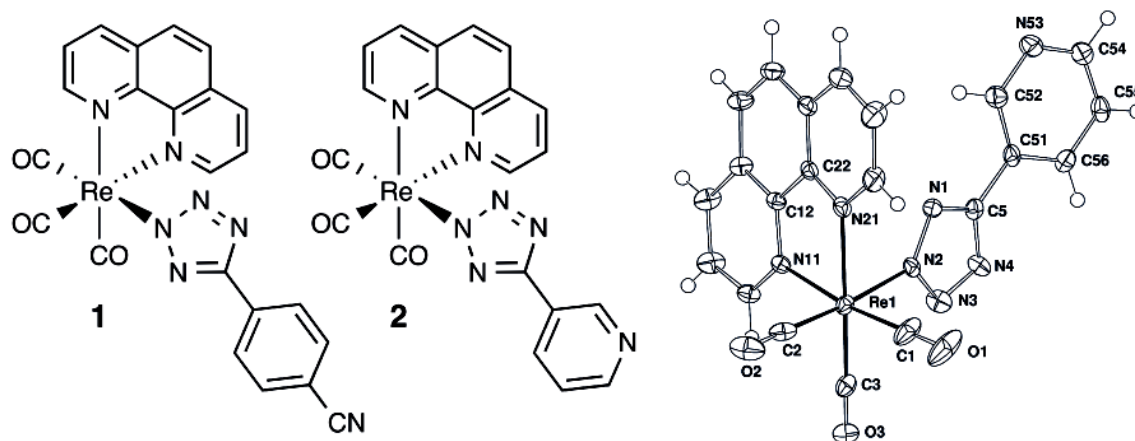


**Figure 1.** Formulations of the Re(I) tetrazolato complexes **1** and **2** used as phosphorescent labels and X-ray crystal structure of **2**, with thermal ellipsoids at the 50% probability level.

Complexes **1** and **2** were prepared according to a previously published procedure,<sup>[36]</sup> via direct exchange of the chloro ligand in *fac*-[Re(CO)<sub>3</sub>(**phen**)Cl], where **phen** = 1,10-phenanthroline, with the corresponding tetrazolato species. The complexes were satisfactorily characterized via IR and NMR spectroscopy as well as elemental analysis. Complex **2** crystallizes in the monoclinic *P2<sub>1</sub>/c* space group (see SI for complete diffraction data and refinement; CCDC 974717) and shows the typical *facial* arrangement of the CO ligands. The tetrazolato ligand coordinates via its N2 atom. In the crystal packing, neighbouring tetrazolato ligands engage in  $\pi$ -stacking interaction with an interplanar distance of *ca.* 3.4 Å, whereas the lone pair of the pyridine ring locks in a vertex-to-face arrangement with the **phen** ligand (N...**phen**  $\approx$  3.0 Å). The X-ray structure of **1** has been reported elsewhere.<sup>[36]</sup>

The photophysical properties of **1** and **2** were measured in air-equilibrated aqueous solutions (*ca.* 10<sup>-5</sup> M), containing 1% DMSO to facilitate solubilization. The combined data are reported in Table 1 and Figure 2, respectively. Both complexes show absorption profiles with intense ligand centred  $\pi$ - $\pi^*$  transitions around 266 nm and charge transfer bands in the 370-380 nm region. The charge transfer transition was ascribed to a metal-to-ligand charge transfer (MLCT; Re  $\rightarrow$  **phen**), mixed with ligand-to-ligand charge transfer character (LLCT; tetrazole  $\rightarrow$  **phen**).<sup>[37]</sup> Upon excitation to the lowest singlet <sup>1</sup>MLCT manifold, a typical broad and structureless emission band, characteristic of the CT nature of the excited state, was observed between 570 and 585 nm for each complex. The excited state is characterized by a relatively long lifetime ( $\tau$ ), suggesting phosphorescent decay from the triplet <sup>3</sup>MLCT state. Indeed, this prolonged excited state lifetime with respect to faster fluorescence makes these complexes also amenable for time-gated detection

techniques to eliminate background endogenous autofluorescence (see SI).<sup>[12,38]</sup> Notably, the lifetime decay of **1** appears to be biexponential, with a major component at 2.373  $\mu\text{s}$  and a minor component (14%) at 575 ns. These values are both longer than the lifetime of complex **2**, which is 277 ns and monoexponential. The same trend is observed for the values of quantum yields ( $\Phi$ ), 10.3% and 1.8% for complexes **1** and **2**, respectively. This difference was interpreted as potential aggregation of complex **1** in the aqueous medium, possibly resulting in less efficient quenching of the  $^3\text{MLCT}$  excited states by molecules of water and oxygen (see SI).

**Table 1** – Photophysical data for the complexes **1** and **2**.

Complex	Absorption	Emission ( $10^{-5}$ M; H <sub>2</sub> O/DMSO 99:1; RT)		
	$\lambda_{\text{max}}[\text{nm}]$ ( $10^4 \epsilon$ [Lmol <sup>-1</sup> cm <sup>-1</sup> ])	$\lambda$ [nm]	$\tau$ [ns] <sup>a</sup>	$\Phi$
<b>1</b>	266 (8.60)	569	575 (14%)	0.103
	378 (0.54)		2,373 (86%)	
<b>2</b>	266 (8.37)	582	277	0.018
	370 (0.34)			

<sup>a</sup> From air-equilibrated solutions at room temperature.

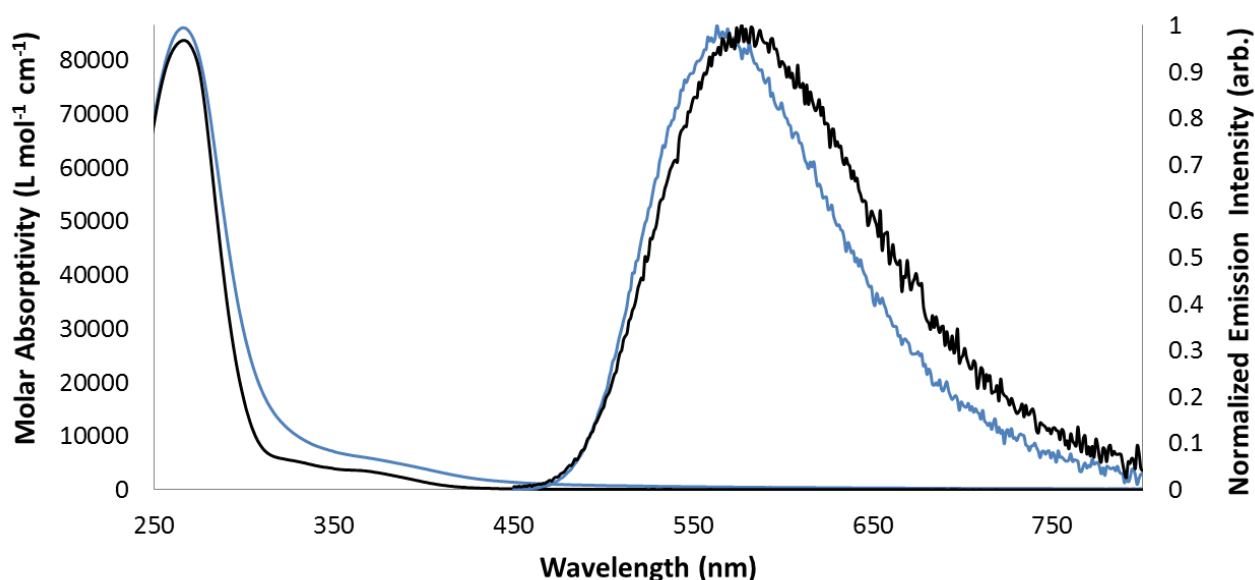


**Figure 2** Absorption and emission profiles of complexes **1** (blue line) and **2** (black line) from a diluted (*ca.*  $10^{-5}$  M) air-equilibrated H<sub>2</sub>O/DMSO 99:1 solution at room temperature.

To investigate the cellular penetration of the complexes **1** and **2**, we employed *Drosophila* larval adipose tissues, which offer distinct advantage for cell biological analysis as it consists of proportionally enlarged cytoplasmic and nuclear areas. The distribution of the complexes was also analysed in human adipose 3T3-L1 cells, with the aim to define the cross-species similarity in their intracellular penetration and distribution. The cells were incubated with 10  $\mu$ M of each complex for 10 minutes at respective permissive temperatures, 25 °C for insect tissue and 37 °C for human cells. The intracellular localization of the complexes was then detected with the use of two-photon excitation, which offers significant advantages for biomedical imaging, given that infrared excitation has a better tissue penetration, reduced out-of-focus photo-bleaching and minimized cellular damage.<sup>[23,38-41]</sup>

As a first step, we optimized excitation wavelength and emission intervals to specifically detect the signal of the Re complexes. Live unstained cells, used as control, and cells stained with either complex **1** or **2** were exposed to two-photon illumination between 770–860 nm. A continuum of images was captured across the emission spectrum between 416–727 nm, with emission increments of 38.9 nm. The strongest signals were obtained upon excitation in the 790-830 nm range, with the brightest emission from the complexes detected within the 533-610 nm wavelength interval (Figure 3, see SI for the complete excitation and emission sections). Under these conditions, minimal endogenous auto-fluorescence was detected in the unstained tissue. This wavelength range corresponds to the emission maxima previously detected for these complexes in solution (Figure 2), suggesting that there is no chemical modification of the complexes in physiologically environment. This is important as anionic ancillary ligands are known to be susceptible to ligand exchange reactions, and this exchange seems to be responsible for the cytotoxicity of probes such as *fac*-[Re(CO)<sub>3</sub>(diim)Cl].<sup>[42]</sup> However, there were no morphological signs of cytotoxicity detected upon 30 min of treatment with complexes **1** or **2**. No evident signs of cytotoxicity could also be detected via MTS assay (see SI).

Importantly, the signal from **1** or **2** was detected within the cells in the first 10 minutes after incubation, indicating that intracellular entry occurs readily and via a mechanism distinct from endocytosis, possibly passive diffusion. A rapid uptake is an extremely desirable attribute for a cellular probe in order to avoid any effect on normal cell physiology and metabolism.<sup>[1]</sup>

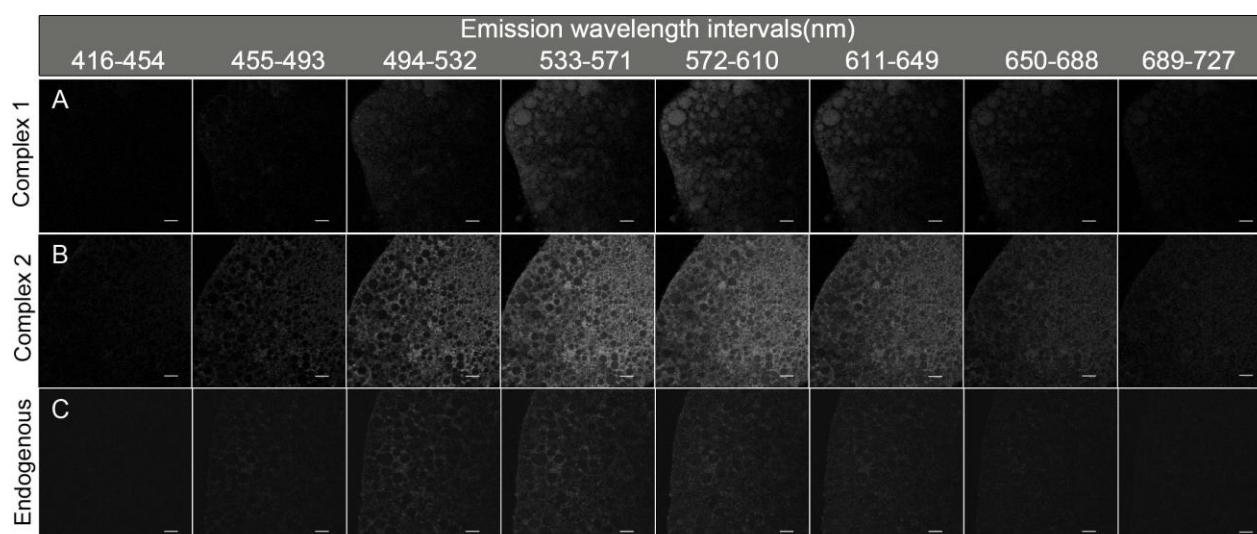


**Figure 3.** Emission fingerprinting of **1** and **2** as compared to endogenous fluorescence in *Drosophila* fat body tissue. Cells were illuminated with two-photon laser at 830 nm. Scale bar = 10  $\mu\text{m}$ .

The micrographs of the *Drosophila* adipose fat body cells (Figure 3) indicate that the complexes **1** and **2** accumulate within specific, yet markedly different, intracellular compartments. To define the organelle specificity, the Re-stained cells as well as differentiated human adipose 3T3-L1 cells were counterstained with four commercially available optical probes, which were specific for; i) acidic endosomes and lysosomes, detected by LysoTracker<sup>®</sup>Green; ii) mitochondria, recognized by Mitotracker<sup>®</sup>Red; iii) organelles containing neutral lipids, detected by Oil Red; and iv) free cholesterol, detected by Filipin. The results are presented in Figures 4 and 5. To discriminate between the signals emitted by the Re complexes or the reference probes, the co-localization analysis was carried out using different spectral intervals, for LysoTracker<sup>®</sup>Green and Mitotracker<sup>®</sup>Red, or spectral unmixing for Filipin (see SI). Due to a significant spectral overlap, Oil Red staining was carried out independently from the complexes **1** and **2**, and conclusion was based on the distinct morphology of the lipid droplets.

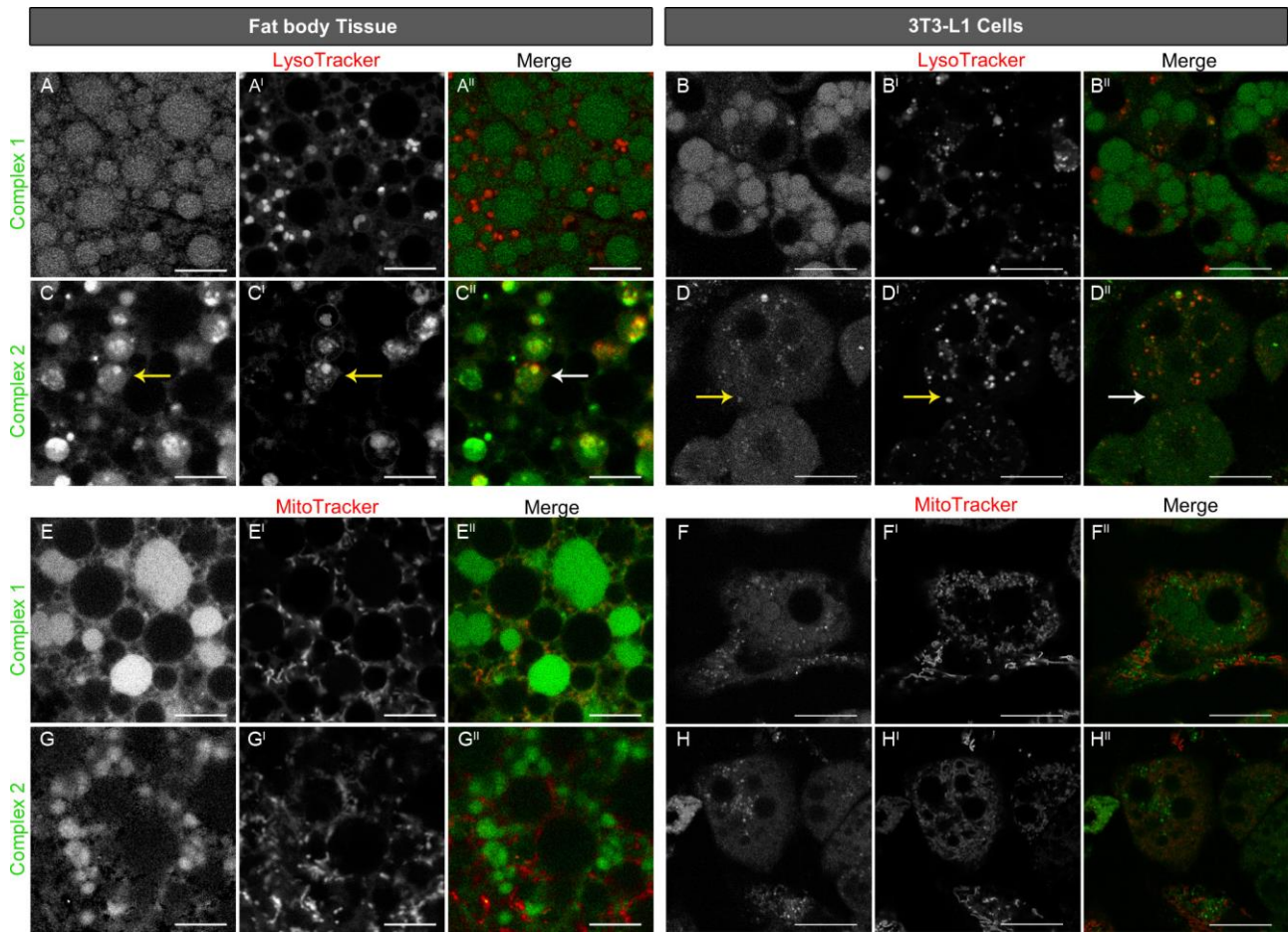


**Figure 4.** Cellular localization of **1** and **2** visualized by two-photon excitation in *Drosophila* fat body and 3T3-L1 cells in relation to late endosomes and mitochondria. Micrographs showing cells stained with **1** (greyscale in A, B, E and F; green in A<sup>II</sup>, B<sup>II</sup>, E<sup>II</sup> and F<sup>II</sup>) or **2** (greyscale in C, D, G and H; green in C<sup>II</sup>, D<sup>II</sup>, G<sup>II</sup> and H<sup>II</sup>). Late acidic endosomes were depicted by staining with LysoTracker<sup>®</sup>Green (greyscale in A<sup>I</sup>, B<sup>I</sup>, E<sup>I</sup> and F<sup>I</sup>; red in A<sup>II</sup>, B<sup>II</sup>, E<sup>II</sup> and F<sup>II</sup>). Mitochondria were depicted by staining with MitoTracker<sup>®</sup>Red (greyscale in C<sup>I</sup>, D<sup>I</sup>, G<sup>I</sup> and H<sup>I</sup>; red in C<sup>II</sup>, D<sup>II</sup>, G<sup>II</sup> and H<sup>II</sup>). Arrows in D/E panels depicts co-localization between **2** and LysoTracker<sup>®</sup>Red positive compartments. Scale bar = 10  $\mu$ m.



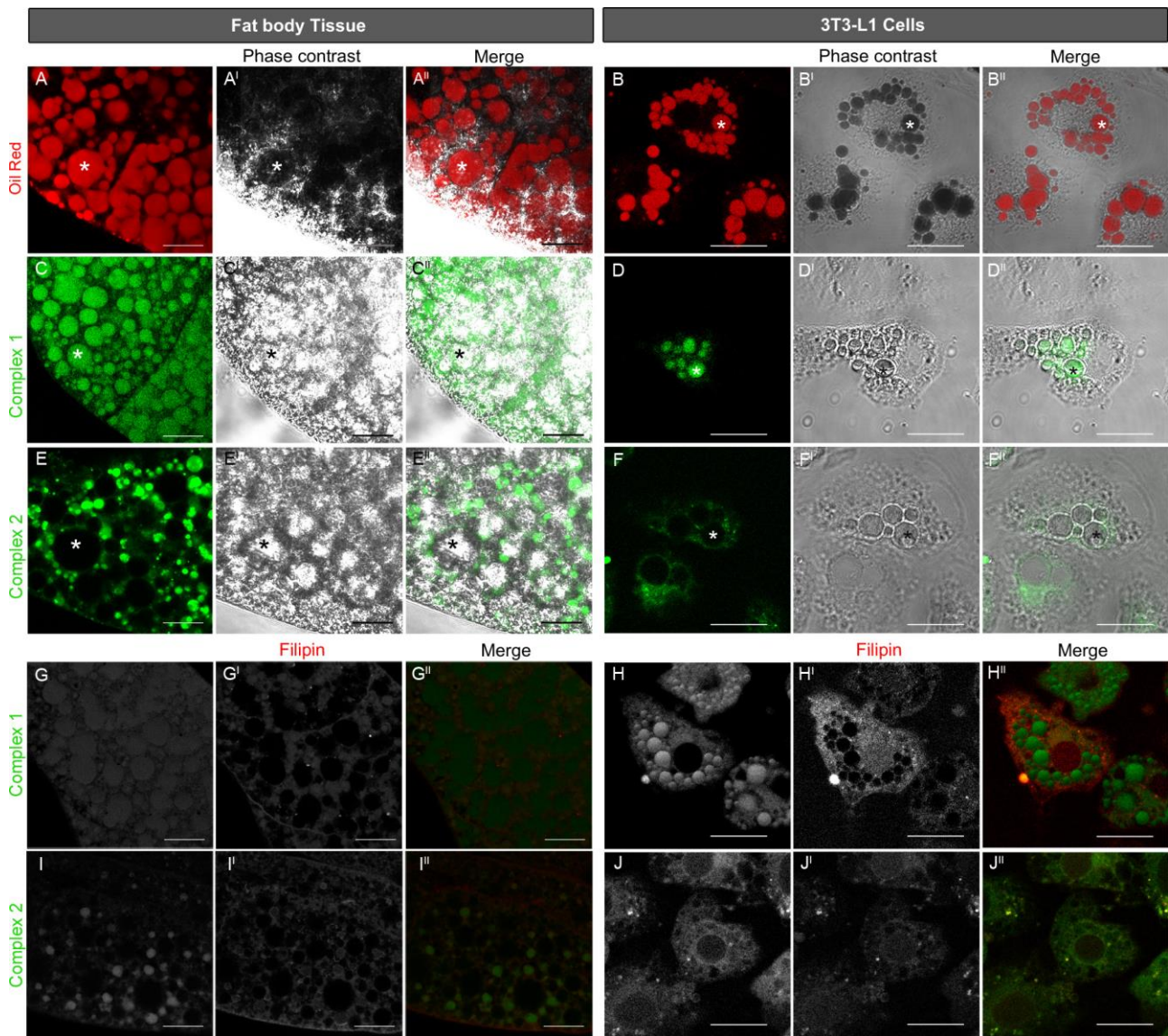


**Figure 5.** Cellular localization of **1** and **2** visualized by two-photon excitation in *Drosophila* fat body and 3T3-L1 cells in relation to lipid droplets and free cholesterol. Micrographs showing *Drosophila* fat body cells (A-A<sup>II</sup>, C-C<sup>II</sup>, E-E<sup>II</sup>, G-G<sup>II</sup>, I-I<sup>II</sup>) and 3T3-L1 matured adipose cells (B-B<sup>II</sup>, D-D<sup>II</sup>, F-F<sup>II</sup>, H-H<sup>II</sup>, J-J<sup>II</sup>). Lipid droplets depicted by staining of fixed cells with Oil Red (red in A and A<sup>II</sup>, B and B<sup>II</sup>). In Phase contrast images, the Oil Red light absorption appears as dark area in lipid droplets (depicted by asterisk in A<sup>I</sup> and B<sup>I</sup>). The signal from **1** (green in C and C<sup>II</sup>, D and D<sup>II</sup>) locates within lipid droplets (depicted by \* in C<sup>I</sup> and D<sup>I</sup>, Phase contrast image), while complex **2** (green in E and E<sup>II</sup>, F and F<sup>II</sup>) is localized outside of lipid droplets (depicted by asterisk in E<sup>I</sup> and F<sup>I</sup>, translucent in Phase contrast image). Free cellular cholesterol detected by staining of fixed cells with Filipin (greyscale in G<sup>I</sup>, I<sup>I</sup>, H<sup>I</sup> and J<sup>I</sup>, red in G<sup>II</sup>, I<sup>II</sup>, H<sup>II</sup> and J<sup>II</sup>). Neither **1** nor **2** showed co-localization with Filipin (greyscale in G, I, H and J, green in G<sup>II</sup>, I<sup>II</sup>, H<sup>II</sup> and J<sup>II</sup>). Scale bar = 20  $\mu$ m



Complex **1** showed no significant signal in organelles containing LysoTracker<sup>®</sup>Green or MitoTracker<sup>®</sup>Red in both cell lines. By contrast, **2** showed co-localization with LysoTracker<sup>®</sup>Green but not with mitochondria stained by MitoTrackerRed<sup>®</sup> (Figure 4). Interestingly, **1** appeared to have stained organelles whose morphology is consistent with that of the lipid droplets (Figure 5C-D), which was confirmed by co-staining of fixed tissues with Oil Red (Figure 5A-B).

From these co-localization studies, it is evident that **1** is an efficient stain for the lipid droplets in live tissues. On the other hand, **2** seems to have a high affinity for acidic organelles, such as late endosome and lysosomes. The different behavior might be rationalized by considering the nature of the ancillary tetrazolato ligand in the two complexes. Complex **1** remains neutral in the cellular environment, as the tetrazolato ligand is too weak as a Brønsted base to undergo protonation. The lack of protonation would confer its high affinity for the neutral lipophilic environment within the lipid droplets. However, **2** is likely to be present in equilibrium with its pyridinium form, which is responsible for the high affinity of the species for organelles characterized by an acidic environment. This conclusion is based on the fact that conventional lysosomal probes contain fluorescent groups coupled with weakly basic amine functionalities. Again, this differential targeting of two distinct cellular organelles implies that the tetrazole ligand does not dissociate from the Re centre within cells, making tetrazolato complexes of tricarbonyl Re(I) diimine cores a robust building block in the design of cellular stains with high specificity. Our results provide evidence of how simple and targeted variations in the chemical nature of metal complexes modulate the specificity of the probe in relation to their organelle localization. This efficient and diverse organelle targeting has been achieved without any conjugation of the metal complex to specific biovectors.

In conclusion, two Re tetrazolato complexes have been investigated for their capacity to serve as cellular labels, and their cellular uptake and intracellular localization suggested a relationship between their structure and specificity for distinct organelles. These studies have utilised two-photon excitation, which has a significant advantage in non-invasive imaging of live cells, while spectral image acquisition allows efficient discrimination between endogenous fluorescence and probe emission. Significantly, these findings open the route to the development of a new generation of phosphorescent and organelle specific dyes for the study of lipid droplets, whose imaging has to date only been achieved with conventional lipophilic fluorophores.

\*\* The authors acknowledge financial contribution from the Australian Research Council (FT1301000033, LE1301000052), Curtin University and the University of South Australia. The time-gated laser and imaging system used in this work was supplied by Quantitative Pty Ltd.

Access to the facilities at the Centre for Microscopy, Characterisation and Analysis, University of Western Australia, is also kindly acknowledged.

## References

- [1] D. Parker, *Aust. J. Chem.* **2011**, *64*, 239–243.
- [2] V. Fernández-Moreira, F. L. Thorp-Greenwood, M. P. Coogan, *Chem. Commun.* **2010**, *46*, 186–202.
- [3] Q. Zhao, C. Huang, F. Li, *Chem. Soc. Rev.* **2011**, *40*, 2508–2524.
- [4] K. K.-W. Lo, A. W.-T. Choi, W. H.-T. Law, *Dalton Trans.* **2012**, *41*, 6021–6047.
- [5] A. J. Amoroso, R. J. Arthur, M. P. Coogan, V. Fernández-Moreira, A. J. Hayes, D. Lloyd, C. Millet, S. J. Pope, *New J. Chem.* **2008**, *32*, 1097–1102.
- [6] R. G. Balasingham, F. L. Thorp-Greenwood, C. F. Williams, M. P. Coogan, S. J. A. Pope, *Inorg. Chem.* **2012**, *51*, 1419–1426.
- [7] N. Viola Villegas, A. Rabideau, J. Cesnavicious, J. Zubieta, R. Doyle, *ChemMedChem* **2008**, *3*, 1387–1394.
- [8] K. K.-W. Lo, T. K.-M. Lee, J. S.-Y. Lau, W.-L. Poon, S.-H. Cheng, *Inorg. Chem.* **2008**, *47*, 200–208.
- [9] D. Maggioni, F. Fenili, L. D'Alfonso, D. Donghi, M. Panigati, I. Zanoni, R. Marzi, A. Manfredi, P. Ferruti, G. D'alfonso, et al., *Inorg. Chem.* **2012**, *51*, 12776–12788.
- [10] K. Lo, W. Hui, C. Chung, K. Tsang, D. Ng, N. Zhu, K. Cheung, *Coord. Chem. Rev.* **2005**, *249*, 1434–1450.
- [11] K. K.-W. Lo, W. H.-T. Law, J. C.-Y. Chan, H.-W. Liu, K. Y. Zhang, *Metallomics* **2013**, *5*, 808–812.
- [12] L. Murphy, A. Congreve, L.-O. Pålsson, J. A. G. Williams, *Chem. Commun.* **2010**, *46*, 8743–8745.
- [13] C. Y.-S. Chung, S. P.-Y. Li, M.-W. Louie, K. K.-W. Lo, V. W.-W. Yam, *Chem. Sci.* **2013**, *4*, 2453–2462.
- [14] R. G. Balasingham, C. F. Williams, H. J. Mottram, M. P. Coogan, S. J. A. Pope, *Organometallics* **2012**, *31*, 5835–5843.
- [15] T. Zou, C. T. Lum, S. S.-Y. Chui, C.-M. Che, *Angew. Chem. Int. Ed.* **2013**, *52*, 2930–2933.
- [16] D. T. Thielemann, A. T. Wagner, E. Rösch, D. K. Kölmel, J. G. Heck, B. Rudat, M. Neumaier, C. Feldmann, U. Schepers, S. Bräse, et al., *J. Am. Chem. Soc.* **2013**, *135*, 7454–7457.
- [17] D. G. Smith, R. Pal, D. Parker, *Chem. Eur. J.* **2012**, *18*, 11604–11613.
- [18] J. W. Walton, A. Bourdolle, S. J. Butler, M. Soulie, M. Delbianco, B. K. McMahon, R. Pal, H. Puschmann, J. M. Zwier, L. Lamarque, et al., *Chem. Commun.* **2013**, *49*, 1600–1602.
- [19] R. G. Balasingham, M. P. Coogan, F. L. Thorp-Greenwood, *Dalton Trans.* **2011**, *40*, 11663–11674.
- [20] E. New, A. Congreve, D. Parker, *Chem. Sci.* **2010**, *1*, 111–118.
- [21] K. Yin Zhang, K. Ka-Shun Tso, M.-W. Louie, H.-W. Liu, K. Kam-Wing Lo, *Organometallics* **2013**, *32*, 5098–5102.
- [22] V. Fernández-Moreira, M. L. Ortego, C. F. Williams, M. P. Coogan, M. D. Villacampa, M. C. Gimeno, *Organometallics* **2012**, *31*, 5950–5957.
- [23] E. Ferri, D. Donghi, M. Panigati, G. Prencipe, L. D'Alfonso, I. Zanoni, C. Baldoli, S. Maiorana, G. D'alfonso, E. Licandro, *Chem. Commun.* **2010**, *46*, 6255–6257.
- [24] C. Mari, M. Panigati, L. D'Alfonso, I. Zanoni, D. Donghi, L. Sironi, M. Collini, S. Maiorana, C. Baldoli, G. D'alfonso, *Organometallics* **2012**, *31*, 5918–5928.

- [25] M.-W. Louie, H.-W. Liu, M. H.-C. Lam, Y.-W. Lam, K. K.-W. Lo, *Chem. Eur. J.* **2011**, *17*, 8304–8308.
- [26] C. A. Puckett, R. J. Ernst, J. K. Barton, *Dalton Trans.* **2010**, *39*, 1159–1170.
- [27] S. Cermelli, Y. Guo, S. P. Gross, M. A. Welte, *Curr. Biol.* **2006**, *16*, 1783–1795.
- [28] D. L. Brasaemle, J. C. Hansen, *Curr. Biol.* **2006**, *16*, R918–20.
- [29] A. S. Greenberg, R. A. Coleman, F. B. Kraemer, J. L. McManaman, M. S. Obin, V. Puri, Q.-W. Yan, H. Miyoshi, D. G. Mashek, *J. Clin. Invest.* **2011**, *121*, 2102–2110.
- [30] N. Kraemer, R. V. Farese Jr., T. C. Walther, *EMBO Mol. Med.* **2013**, *5*, 973–983.
- [31] M. Digel, R. Ehehalt, J. Füllekrug, *FEBS Letters* **2010**, *584*, 2168–2175.
- [32] C. Thiele, J. Spandl, *Curr. Opin. Cell Biol.* **2008**, *20*, 378–385.
- [33] A. S. Greenberg, M. S. Obin, *Cell Metab.* **2008**, *7*, 472–473.
- [34] R. V. Farese Jr., T. C. Walther, *Cell* **2009**, *139*, 855–860.
- [35] L. Kuerschner, C. Moessinger, C. Thiele, *Traffic* **2008**, *9*, 338–352.
- [36] P. J. Wright, S. Muzzioli, M. V. Werrett, P. Raiteri, B. W. Skelton, D. S. Silvester, S. Stagni, M. Massi, *Organometallics* **2012**, *31*, 7566–7578.
- [37] M. V. Werrett, D. Chartrand, J. D. Gale, G. S. Hanan, J. G. MacLellan, M. Massi, S. Muzzioli, P. Raiteri, B. W. Skelton, M. Silberstein, et al., *Inorg. Chem.* **2011**, *50*, 1229–1241.
- [38] S. W. Botchway, M. Charnley, J. W. Haycock, A. W. Parker, D. L. Rochester, J. A. Weinstein, J. A. G. Williams, *Proc. Natl. Acad. Sci.* **2008**, *105*, 16071–16076.
- [39] G. Masanta, C. S. Lim, H. J. Kim, J. H. Han, H. M. Kim, B. R. Cho, *J. Am. Chem. Soc.* **2011**, *133*, 5698–5700.
- [40] W.-S. Lo, W.-M. Kwok, G.-L. Law, C.-T. Yeung, C. T.-L. Chan, H.-L. Yeung, H.-K. Kong, C.-H. Chen, M. B. Murphy, K.-L. Wong, et al., *Inorg. Chem.* **2011**, *50*, 5309–5311.
- [41] C.-L. Ho, K.-L. Wong, H.-K. Kong, Y.-M. Ho, C. T.-L. Chan, W.-M. Kwok, K. S.-Y. Leung, H.-L. Tam, M. H.-W. Lam, X.-F. Ren, et al., *Chem. Commun.* **2012**, *48*, 2525–2527.
- [42] A. J. Amoroso, M. P. Coogan, J. E. Dunne, V. Fernández-Moreira, J. B. Hess, A. J. Hayes, D. Lloyd, C. Millet, S. J. A. Pope, C. Williams, *Chem. Commun.* **2007**, 3066–3068.